

Genesis of the Blende Carbonate-Hosted Zn-Pb-Ag Deposit, North-Central Yukon Territory: Geologic, Fluid Inclusion and Isotopic Constraints

MICHELLE ROBINSON AND COLIN I. GODWIN

Department of Geological Sciences, The University of British Columbia, Vancouver, British Columbia, Canada V6T 1Z4

Abstract

The Blende zinc-lead-silver deposit, 60 km northeast of Keno City, Yukon Territory, is spatially associated with a mid-Proterozoic fault zone that crosscuts stromatolitic dolostones of the Middle Proterozoic, upper Gillespie Lake Group. It is the largest known strata-bound, carbonate-hosted, zinc-lead deposit in the Yukon Territory. Mineralization, largely epigenetic, consists of sphalerite and galena, with lesser pyrite and chalcopyrite, and trace fribergite in quartz-carbonate veins and veinlets. Veining is zoned from copper- and silver-rich mineralization at the base of the deposit, through lead- and zinc-rich, to zinc-dominated at the top. Detailed cross-section mapping indicates that controls on the deposit are both stratigraphic and structural. Many of the stromatolite beds are mineralized and are especially rich in lead and zinc close to normal faults. Fluid inclusion studies indicate that mineralizing fluids were about 285°C during main-stage mineralization.

Sulfur isotope analyses of unmineralized whole-rock samples cluster tightly around an average $\delta^{34}\text{S}$ value of 23.6 ± 0.4 per mil. The source of sulfur is apparently seawater sulfate, probably from minor anhydrite in the host dolostone. Sulfide sulfur isotope ratios define three populations. Local blebs of pyrite associated with stromatolites have markedly negative ratios (-15.1%) that are probably bacteriogenic in origin. Vein sulfides in tight dolostones have ratios between 19.0 and 26.3 per mil, with an average $\delta^{34}\text{S}$ value of 23.2 ± 0.9 per mil. This is virtually identical to the whole-rock sulfur isotope ratio. Veins that crosscut stromatolitic beds have sulfur isotope ratios between 18.3 and 7.4 per mil with a mean of 15.0 ± 1.2 per mil. Intermediate sulfur isotope ratios apparently reflect a mixed sulfur source of both whole-rock sulfate and biogenic sulfide.

Carbon and oxygen isotopes in host rocks and ore-stage dolomite spar are related genetically; both are related to ancient seawater. The calculated isotopes for mineralizing fluids are characteristic of basinal brines.

Galena lead isotopes, interpreted using the shale model, indicate an age of 1.4 to 1.5 Ga for the deposit. This is older than, or penecontemporaneous with, regionally extensive diorite sills (1380 ± 4 Ma, U-Pb zircon) that occur below the upper Gillespie Lake Group. However, a close spatial association of mineralization to upper parts of sills and the high temperature of ore fluids from fluid inclusion homogenization temperatures supports a genetic relationship between the sills and mineralization.

Introduction

THE Blende zinc-lead-silver deposit is about 60 km northeast of Keno City in north-central Yukon Territory (Fig. 1: NTS 106D, $64^\circ 24' \text{N}$ and $134^\circ 40' \text{W}$, elev 1,130–1,875 m). It is the largest known strata-bound carbonate-hosted sphalerite and galena deposit in the Yukon Territory. Mineralization is hosted by upper Gillespie Lake Group dolostone, a Middle Proterozoic unit within the Wernecke Supergroup that forms a 100-km-wide band across north-central Yukon (Fig. 1, inset). Access to the Blende deposit during the summer season is by helicopter from the Sadie expediting camp 5 km north of Keno City. During the winter the property can be reached by the Wind River trail, an established winter road. The Blende is centered near Mount Williams, a distinctive peak in the southern Wernecke Mountains. Pleistocene to Recent glaciation has modified the terrain; slopes are mostly oversteepened and cirques are common above 1,370 m.

Property at the Blende was first staked in 1975 as the Will claims by the Cyprus Anvil Mining Corporation to cover a geochemical stream sediment anomaly. Archer, Cathro and Associates (1981) Ltd. restaked the prospect

as the Blende claims in 1981. Work continued sporadically until 1986 when NDU Resources Ltd. acquired the claims and initiated a drill program in 1988 consisting of three holes totaling 718 m. In 1989 the deposit was optioned to Billiton Metals Canada, Inc., for a 50 percent interest. Drilling programs in 1990 and 1991 were operated by Billiton with field management by Archer, Cathro and Associates. Reserves currently outlined by 20,000 m of diamond drilling are 20 Mt of ore grading 6 percent Zn + Pb.

This paper presents the results of detailed geologic section mapping and sampling. Petrographic, fluid inclusion, and stable isotope analyses were done on many hand and drill core samples. Galena lead isotopes were used to date mineralization. U-Pb analysis of zircons from a coarse-grained diorite sill determined the age of spatially and probably genetically related intrusions.

Regional Stratigraphic Setting

The Blende deposit is hosted by the Wernecke Supergroup (Fig. 1), a Middle to Late Proterozoic shelf assemblage deposited during periodic extension at the margin of ancestral North America (Thompson et al., 1986). The

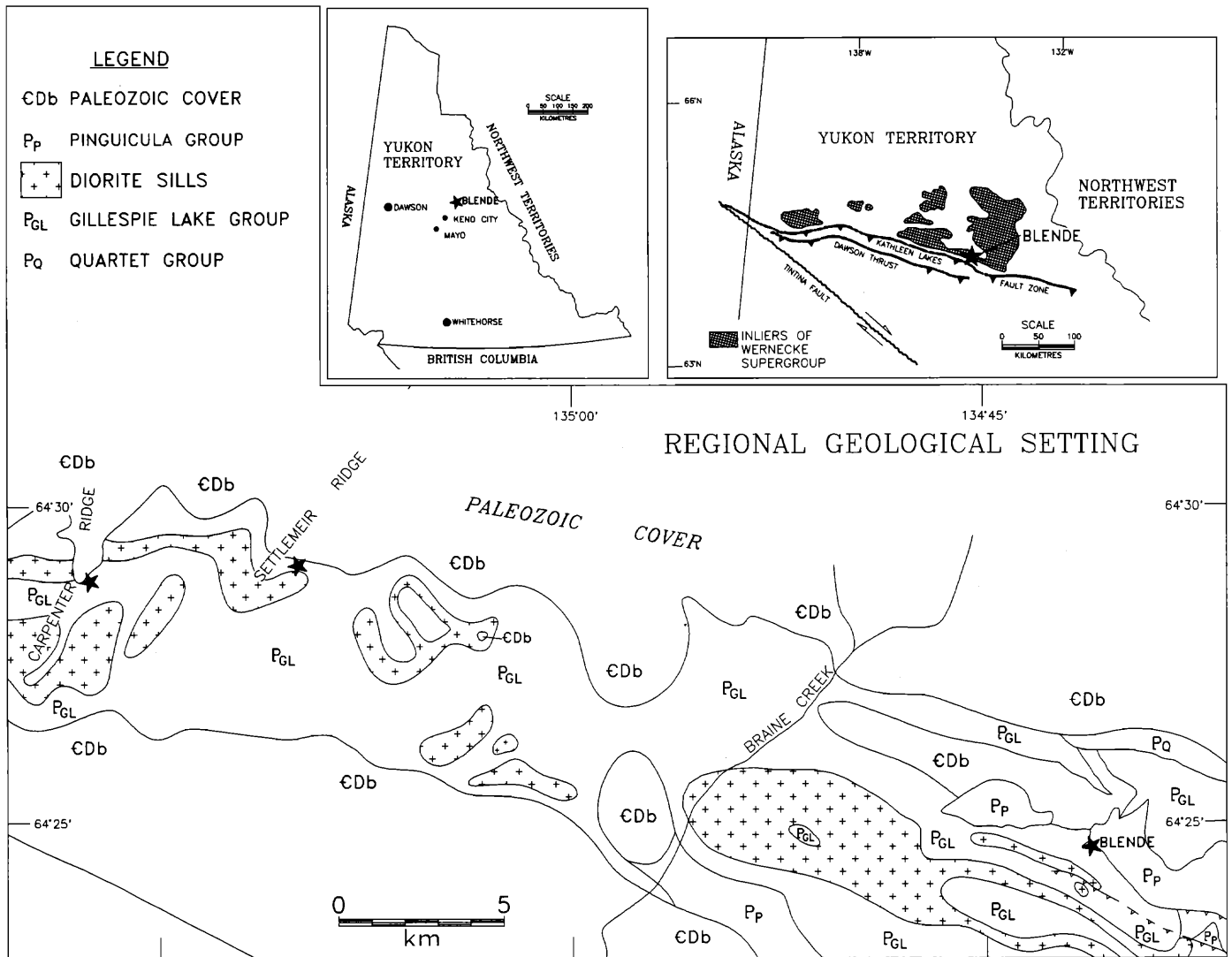


FIG. 1. Location and regional geologic setting of the Blende carbonate-hosted zinc-lead deposit (from Roots, 1990, after Green, 1972), north-central Yukon Territory. Stars show the location of important zinc-lead occurrences.

Wernecke Supergroup has been subdivided into three units: the Fairchild Lake Group, the Quartet Group, and the Gillespie Lake Group. Extension after deposition of the Gillespie Lake Group opened subbasins that filled with Late Proterozoic sediment. These may correlate with the Pinguicula Group sequences of the Mackenzie Supergroup that overlies the Wernecke Supergroup (Eisbacher, 1981). Paleozoic carbonates unconformably overlie the Proterozoic succession. Diorite dikes and sills intrude only the Proterozoic rocks, indicating a pre-Paleozoic age. Late Mesozoic folding and thrusting has formed a west-trending belt that extends from Alaska to the Northwest Territories (Roots, 1990). Only Proterozoic units are described below.

Fairchild Lake Group

The Fairchild Lake Group, not exposed in the vicinity of the Blende deposit, is the oldest unit of the Wernecke

Supergroup. It comprises pale gray-weathering siltstone, mudstone, and fine-grained sandstone with minor intercalated carbonate (Delaney, 1981), which probably was deposited mainly in deep water. However, carbonate horizons immediately north of the present-day Wernecke Mountains indicate shallower deposition. These rocks, regionally metamorphosed to greenschist facies, locally have been transformed to slates, phyllites, and schists.

Quartet Group

The Quartet Group (Figs. 1 and 2) conformably overlies the Fairchild Lake Group and consists of a monotonous succession of dark gray-weathering siltstone, mudstone, and fine-grained sandstone that have been metamorphosed to slate, phyllite, and schist with minor interbedded quartzite. At the base of the Quartet Group, sedimentary rocks are finer grained, carbonaceous and pyritic, indicating that they probably accumulated in a

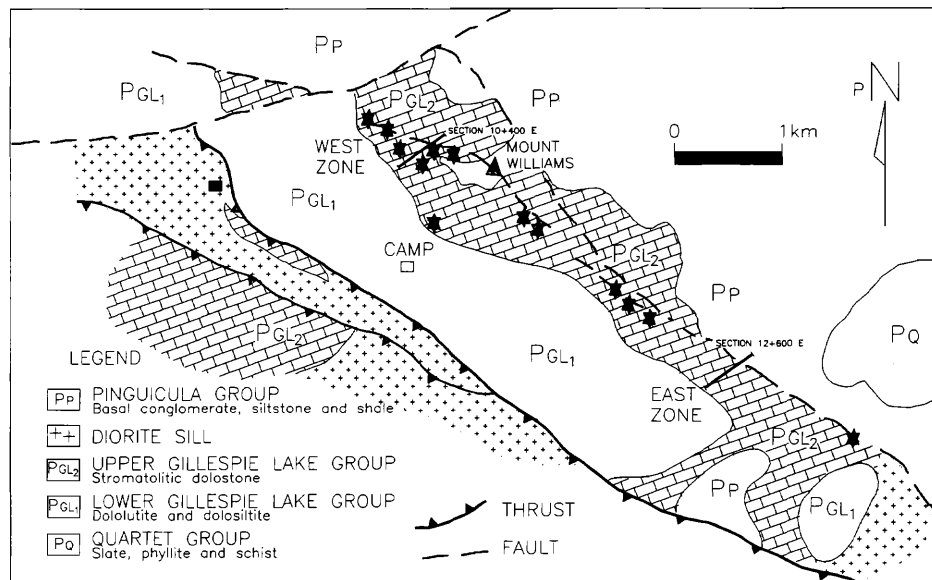


FIG. 2. Blende property geology, Yukon Territory. Stars show outcrops of Zn-Pb mineralization that follows the surface trace of a major normal fault. Filled square shows location of sample collected for U-Pb zircon date.

sediment-starved basin. Upward they merge transitionally into rhythmically layered siltstone and mudstone turbidites (Roots, 1990; Delaney, 1981). The top of the Quartet Group is characterized by fine-grained sandstone with abundant primary sedimentary structures indicative of shallow-marine environments (Delaney, 1981).

Gillespie Lake Group

The Gillespie Lake Group (Figs. 1 and 2) is generally in gradational contact with the underlying Quartet Group (Delaney, 1981; Mustard et al., 1990; Roots, 1990). However, in the Ogilvie Mountains, 100 km west of the study area, Roots (1990) describes large-scale folding and intense deformation of the Quartet Group and an overlying angular unconformity. This indicates that deformation and metamorphism of the Quartet Group must have occurred before deposition of the Gillespie Lake Group. The Gillespie Lake Group in Figure 2 is divided into a lower unit (PGL₁) and an upper unit (PGL₂).

Lower Gillespie Lake Group: This unit consists of 1- to 5-m-thick, fining-upward cycles of brown to dark gray dololite and orange-weathering dolosiltite. Finer grained beds are generally graphitic and contain abundant blebs of pyrite. Microscopic grains of secondary muscovite and chlorite indicate weak regional metamorphism. Sedimentary structures at the base of this division are similar to those found at the top of the Quartet Group. These indicate deposition in a shallow-marine environment (Delaney, 1981) that generally is subtidal and probably sub-wave base (Mustard et al., 1990).

Upper Gillespie Lake Group: This unit (G₂, Figs. 3 and 4) is characterized by the appearance of stromatolitic carbonate. This reflects a change from the deeper water depositional environment of the lower unit to emergent conditions. The stromatolites mostly form the tops of cyclical

shallowing-upward carbonate sedimentary sequences. Details of these cycles are described in the local geology section. The cyclic repetition of these shallowing-upward sequences probably reflects alternating periods of carbonate platform buildup and exposure.

Pinguicula Group

The Pinguicula Group (unit 4 of Roots, 1990) is dominated by dark gray siltstone and dark shales, with interbeds of sandstone and carbonate. A widespread basal conglomerate layer, it disconformably overlies unit PGL₂. This unit was most likely deposited in extensional basins after the deposition of the upper Gillespie Lake Group (Roots, 1990).

Diorite dikes and sills: They are of medium- to coarse-grained hornblende diorite with diabasic texture and intrude all Proterozoic units (Figs. 1 and 2). Large sills greater than 100 m thick form massive cliff-forming units that trend northwest through the Blende property. Small sills and dikes, on the order of 15 m thick, are recessive weathering. All small dikes and sills intruding carbonate rocks are surrounded by pale white-green dedolomitization halos enriched in calcite and serpentine. Larger sills alter and silicify the host dolostone (the lower Gillespie Lake Group unit and the lower parts of the upper unit) to a green rock without destroying primary textures such as bedding. Large mineralized calcite veins in the green dolostone immediately above a major sill may be dewatering structures, implying that the more shale rich sediments may not have been lithified at the time of intrusion. Uranium-lead dating of zircons recovered from a coarse-grained sample of the large sill about 2 km northwest of camp (filled square, Fig. 2) gave an age of 1380 ± 5 Ma (M.L. Bevier, Geological Survey of Canada, pers. commun., 1992).

Middle Proterozoic Geology of the Blende Deposit

Lead-zinc-silver mineralization is hosted by upper Gillespie Lake Group dolostone (Fig. 2). It is spatially associated with a Middle Proterozoic fault zone that strikes about 110° and dips steeply southwest. Most faults in this zone have reverse offset of only a few meters. Figure 2 shows the linear distribution of surface mineral occurrences that parallel these faults for 6 km. Two large mineralized bodies, the west and east zones, have been delineated.

Unit PGL₂ is well exposed on steep slopes and cliffs near the peak of Mount Williams (Fig. 2). Where mineralized, unit PGL₂ tends to be recessive; it is covered by blocky talus in the west zone and glacial till in the east zone. Beds within the unit strike approximately 55° and dip moderately southeast. They are composed of interbedded dololutes, dolosiltites, and dolarenites. Petrographic and X-ray analyses indicate that the sediments are primarily slightly ferroan dolomite with minor quartz and clays. Soft-sediment deformation structures are common; abundant stylolites indicate significant pressure solution. Stromatolitic horizons with lesser oolite- and pisolite-rich beds punctuate the stratigraphy. Typically these strata are arrayed in repeated 5- to 20-m-thick shallowing-upward sequences. Each sequence, where all the units are present, consists of a basal layer of dolosiltite or dololite grading upward into dolarenite that is overlain by undulose cryptalgal laminates passing upward into columnar stromatolites capped by laterally linked domal stromatolites. Some interbedded dolosiltite-lutite horizons contain desiccation cracks, and more rarely, syneresis cracks. Beds of rectangular to subrounded rip-up clasts or intraclast breccias are common. Many of the clasts are cryptalgal dolostone that occurs above or below stromatolite beds and as fill between domal stromatolites. Some cycles do not contain stromatolites at the top of the sequence; in these the cap is formed by thick dolarenite beds containing patches of silicified oolite and pisolite. Patchy silicification of stromatolite layers is frequent and may be a result of early diagenesis (A. Donaldson, Carlton University, pers. commun., 1991). Similarly, silicified patches in the dolarenite horizons indicate that much of the dolarenite present was originally oolitic; original spheroidal textures were lost during diagenesis or dolomitization. On the Blende property, some oolitic and pisolitic horizons are well preserved due to pervasive silicification. These and some stromatolite beds provide useful markers for determining stratigraphic correlations and fault offsets.

Abundant stromatolites are indicative of a warm environment probably conducive to evaporite formation. No extensive evaporite beds were noted on the Blende property, but hand samples containing salt casts were found in talus.

Representative cross sections of the west (10 + 400 E) and east (12 + 600 E) zones are in Figures 3 and 4; their map locations are shown in Figure 2. Southwesterly dipping fractures in Figures 3 and 4 are probably mid-Proterozoic and synmineral. A low-angle southwest-dipping

thrust fault that parallels the sill in Figure 4 is probably related to Mesozoic contraction (Roots, 1990); it cross-cuts early faults. Lithologic correlation and reconstruction of paleogeographic depositional environments was not attempted because rapid facies changes typical of shallow-water carbonate environments make this impossible with drill hole spacing normally at about 100 m. However, at least eight laterally continuous and distinctive markers were identified. Because some of the high-grade zinc-lead mineralization preferentially follows specific stromatolitic beds, the markers are described below for each zone.

West zone markers (section 10 + 400 E)

Marker A: This is a 1.6-m-thick bed of sphalerite-rich stromatolites (Fig. 3, hole 91-47). Although not known to form a continuous marker, it contains high metal values of 16 percent zinc, 4.3 percent lead, and 157 g silver/t. Stromatolites in this bed are columnar and form small club shapes, about 10 cm tall and 5 cm wide.

Marker B: This marker (Fig. 3, holes 91-47 and 91-45) consists of a basal layer of ooids 0.5 mm in diameter that coarsen upward into pisoids 7 mm in diameter. Stromatolites of uncertain morphology form a 2- to 3.5-m-thick cap over the pisoids.

Marker C: This marker (Fig. 3, holes 91-47 and 91-45) is 45 cm thick and contains tiny ooids less than 0.25 mm in diameter at the bottom that grade upward into pisoids reaching 7 mm in diameter. It is overlain (in drill hole 91-45) by a 2.1-m-thick stromatolite bed. Stromatolites are columnar, club shaped, and 10 to 30 cm high with diameters of about 10 cm. Strata-bound galena and sphalerite mineralization grades about 9 percent lead, 1 percent zinc, and 308 g silver/t.

Marker D: This marker (Fig. 3, holes 91-57 and 91-47) is a 1.5- to 3.5-m-thick bed of massive gray dolarenite with occasional intraclasts and local silicified oolite patches. Ooids are unsorted and range from 0.25 to 2 mm diam.

Marker E: It consists of a distinctive sequence of interbedded dolarenite, oolite, dolosiltite, and dololite (Fig. 3, holes 91-57, 91-47, and 91-45). At the base it consists of a 1.5- to 3.5-m-thick section of interbedded dolosiltite and dolarenite with silicified oolite patches. It is likely that all the dolarenite was originally oolitic; however, only where silicification occurs have original textures been preserved. The ooids are poorly sorted and range from 0.25 to 2 mm in diameter. Overlying the basal unit is a 2- to 2.5-m-thick section of dark to medium gray, normally graded, thinly bedded dolosiltite and dololite with a thin central layer of rip-up clasts. The top of the marker consists of 1.5 m of interbedded dolosiltite, dolarenite, and silicified oolite patches.

East zone markers (section 12 + 600 E)

Marker F is a well-preserved shallowing-upward sequence of dolosiltite, oolite, pisolite, and stromatolites (Fig. 4, holes 91-25, 91-41, and 91-22). At the base, it is composed of medium gray dolosiltite overlain by a mostly

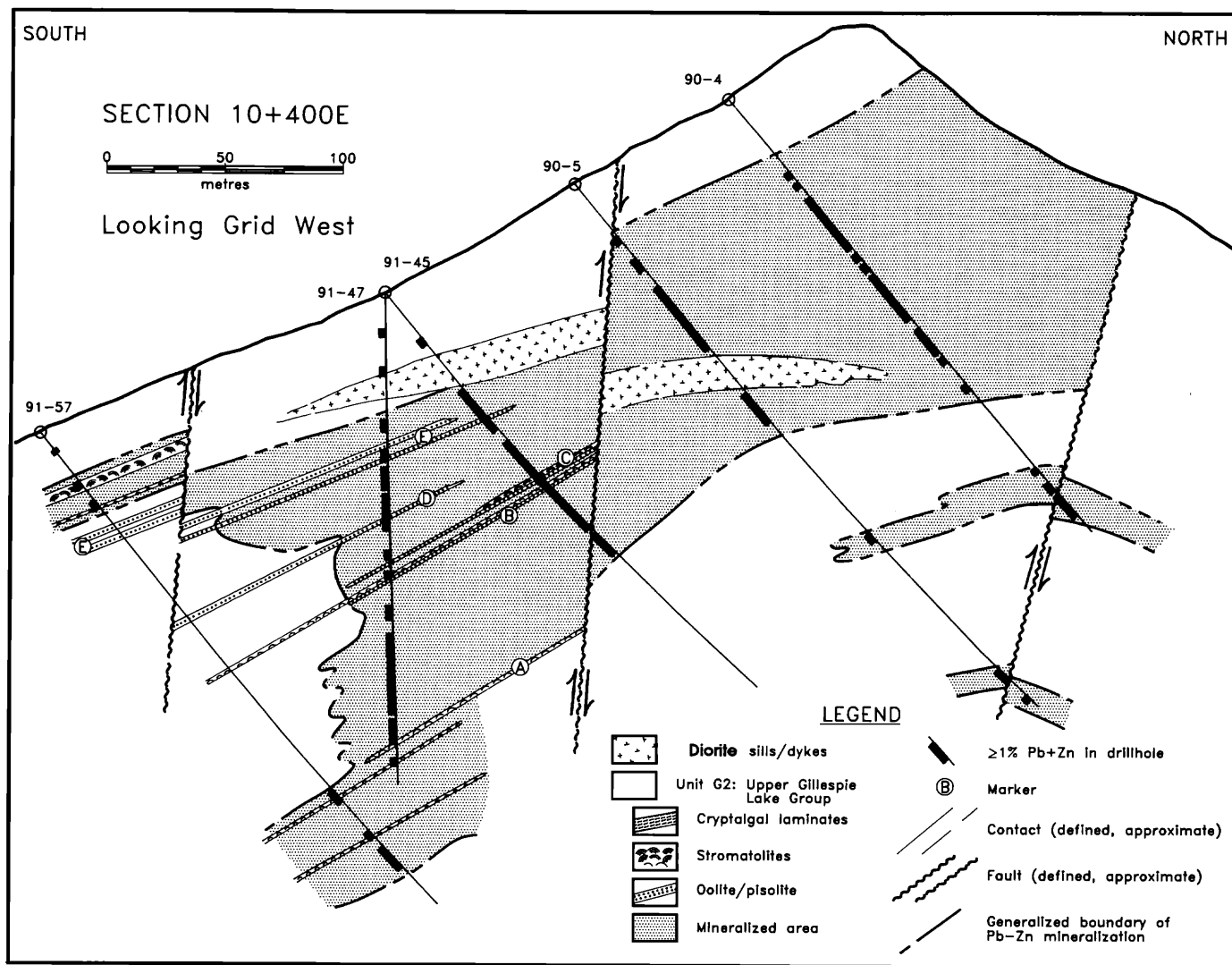


FIG. 3. Geologic cross section of the west zone (section 10 + 400 E, Fig. 2) showing marker beds A to E, Blende property, Yukon Territory. A = sphalerite-rich stromatolitic dolostone. B = coarsening-upward oolite overlain by stromatolites. C = coarsening-upward oolite overlain by club-shaped stromatolites. D = medium gray dolarenite with silicified oolite patches. E = interbedded oolitic dolarenite and dolosiltite.

silicified oolite bed about 1 m thick. In drill hole 91-25, the oolite bed has undergone patchy silicification. These silicified patches contain unsorted ooids and pisoids up to 5 mm in diameter. To the northeast (holes 91-41 and 91-22), the oolite occurs as two coarsening-upward layers in which silicification is pervasive. Stromatolites of variable morphology and thickness cap the sequence. Toward the southwest (hole 91-25) stromatolites are larger than the diameter of the NQ drill core and they form a bed 2 m thick. In hole 91-41, the stromatolites merge laterally into smaller digitate forms up to 2 cm in height; the thickness of the bed decreases to 70 cm. However, a stylolite that cuts through this layer just above the oolite contact may have removed part of this horizon. Farther northeast (hole 91-22) the stromatolite layer merges laterally into undulose cryptalgal laminates.

Marker G: This is a 5.5-m-thick bed of sphalerite-rich

stromatolitic dolosiltite (intersected once by hole 91-19 and twice by hole 91-25, Fig. 4). At the base of the section, stromatolites form undulose cryptalgal laminates that pass upward into digitate forms. The exact geometry of these stromatolites is difficult to determine due to the small size of the drill core compared to the size of the stromatolites. Sulfides present are mainly sphalerite and galena, with lesser amounts of pyrite. Grades of zinc and lead are about 4 and 1.5 percent, respectively.

Marker H: This is the most distinctive marker unit identified in the east zone (intersected in holes 91-19, 91-41, and twice in 91-25, Fig. 4). It averages 6.5 m in thickness and is characterized by pyrite- and galena-rich stromatolites. It contains an average of 25 percent pyrite, 4.1 percent lead, and 2.9 percent zinc in drill holes 91-19 and 91-25. Hole 91-41 just contains pyrite. The morphology of the stromatolites varies in a consistent manner through-

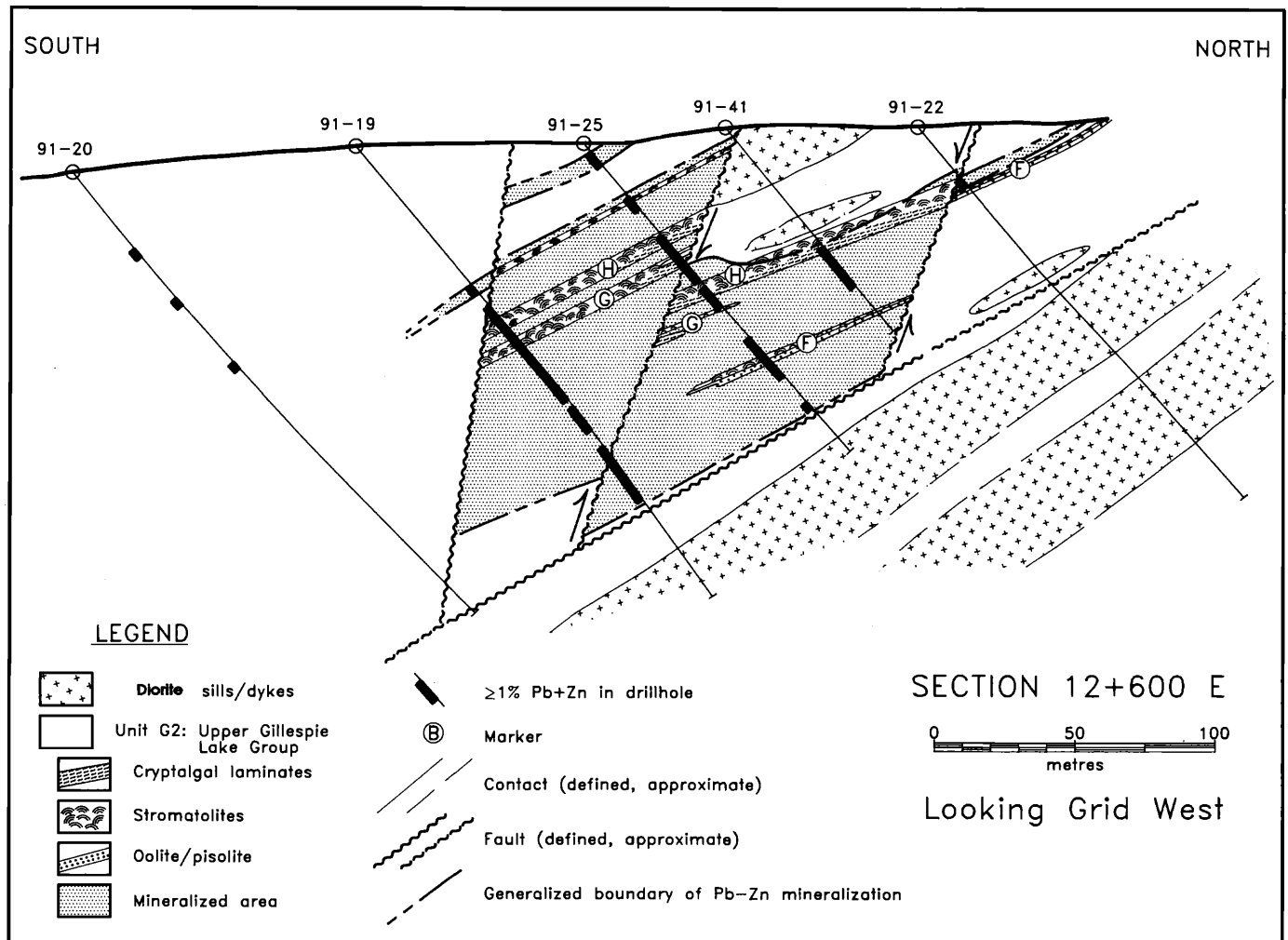


FIG. 4. Geologic cross section of the east zone (section 12 + 600 E, Fig. 2) showing marker beds F to H, Blende property, Yukon Territory. F = coarsening-upward oolite overlain by stromatolites. G = sphalerite-rich stromatolitic dolostone. H = pyrite-rich stromatolitic dolostone.

out the section. To the southwest (holes 91-19 and 91-25) small columnar club-shaped stromatolites up to 20 cm tall and 5 to 10 cm in diameter dominate this marker. To the northeast (hole 19-41), the stromatolites are somewhat smaller, generally reaching dimensions of only 5 by 2 cm; they are underlain by undulose cryptalgal laminates.

Mineralization

Main-stage mineralization occurs discontinuously along a 6-km linear trend following the Middle Proterozoic fault zone defined in Figure 2. In general, sulfides occur as discordant veins (Fig. 5A) and vein breccias (Fig. 5B) along the fault zone, and as concentrations within the stromatolitic horizons of the upper Gillespie Lake Group. The sulfide assemblage in the veins is dominantly sphalerite and galena with lesser pyrite (Fig. 5C). Chalcopyrite and freibergite occur as minor phases in the west zone. Thin envelopes of brucite alteration occur in most veins throughout the deposit. Anglesite, covellite, and smith-

sonite are also present in minor amounts at the top of the west zone where mineralization is weathered.

Paragenesis of most veins is brucite in vein envelopes, sphalerite + galena + pyrite on the selvages of the vein, and sparry dolomite with or without quartz in the core of veins greater than 0.5 cm wide (Fig. 5C). Freibergite and/or chalcopyrite, where present as in the west zone mineralization, are intergrown with sphalerite and galena (Fig. 5D). Late pyrite-rich veins crosscut earlier lead-zinc mineralization.

A more complicated paragenesis of minerals is present in stromatolitic horizons that are crosscut by veins (Fig. 6A). Pyrite and sphalerite botryoids associated with the growth of cryptalgal laminates (Fig. 6B and C; algal mineralization) form the first generation of sulfides. Later galena, sphalerite, and pyrite (and copper sulfides in the basal part of the west zone) replace the original syngenetic sulfides (Fig. 6D). In some cases, sulfides completely replace the original algal laminate (Fig. 6E).

The Blende deposit is crudely zoned from spotty cop-

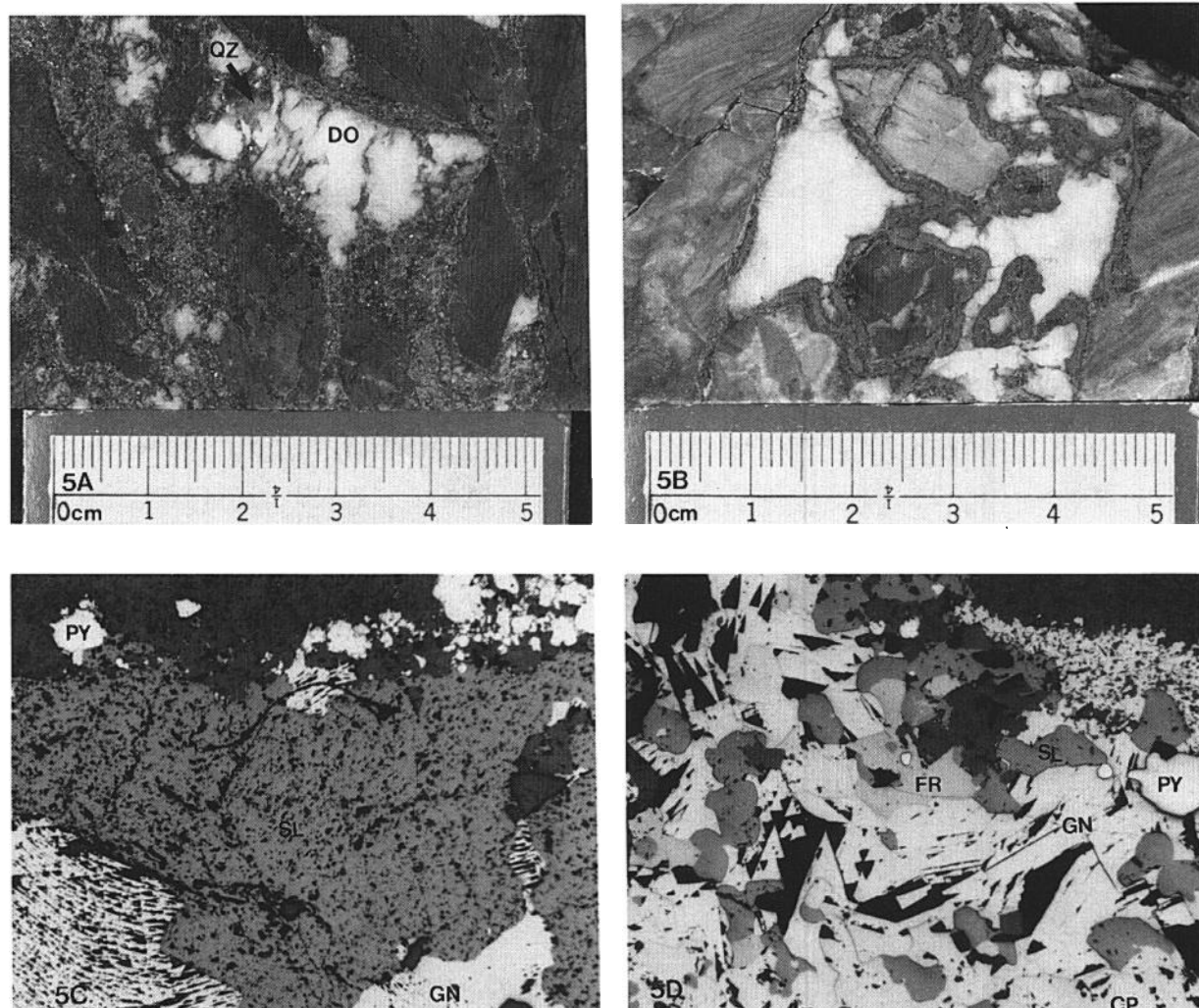


FIG. 5. Photographs of rocks and polished thin sections, Blende property, Yukon Territory. A. Typical mineralized vein in medium gray dolosiltite (hole 91-19, 123.6 m). Pyrite, galena, and sphalerite occur intergrown together on the edge of the vein. Dolomite (DO) and quartz (QZ) occur in the center. B. Vein breccia (20 + 100 N, 12 + 700 E) contains sphalerite, pyrite, and lesser galena that rims fragments. C. Photomicrograph of a typical vein (hole 91-25, 93.5 m; reflected light). Vein contains pyrite (PY) and galena (GN) toward the edges, and sphalerite (SL) in the center. D. Photomicrograph of typical copper rich mineralization that occurs sporadically at the base of the west zone (hole 91-60, 262.14 m; reflected light). Vein contains galena (GN), chalcocopyrite (CP), sphalerite (SL), frieberrite (FR), and pyrite (PY).

per- and silver-rich mineralization at the base of the west zone, through lead-rich mineralization in the middle and upper levels of the zone. Zinc-rich mineralization is dominant in the east zone. High-grade mineralization is mostly strata bound within stromatolitic horizons throughout the deposit (Figs. 3 and 4).

Fluid Inclusions

A general fluid inclusion study using standard heating techniques was done on five doubly polished thin sections from typical ore in the Blende deposit. Inclusions in sphalerite were emphasized although quartz and dolomite were also examined. Results of 21 runs are given in Table 1, which also contains analytical details.

Fluid inclusions in sphalerite and quartz range from 3

to 50 μm in diameter. They are liquid dominant and contain a vapor phase. Inclusions in dolomite are similar but tend to be smaller (less than 10 μm). No daughter crystals were present in any of the fluid inclusions. Most sphalerite and dolomite, however, is recrystallized. Recrystallization is most likely due to regional lower greenschist facies metamorphism. Abundant planes of small inclusions within all minerals might reflect this event. The emphasis here was on identifying and measuring primary fluid inclusions related to mineralization using criteria from Roedder (1984). The small inclusions in dolomite were not homogenized.

Primary fluid inclusions are found in subparallel growth zones in a zoned sphalerite crystal protruding into the center of a vein (Table 1, samples MR1SL-P to MR6SL-P).

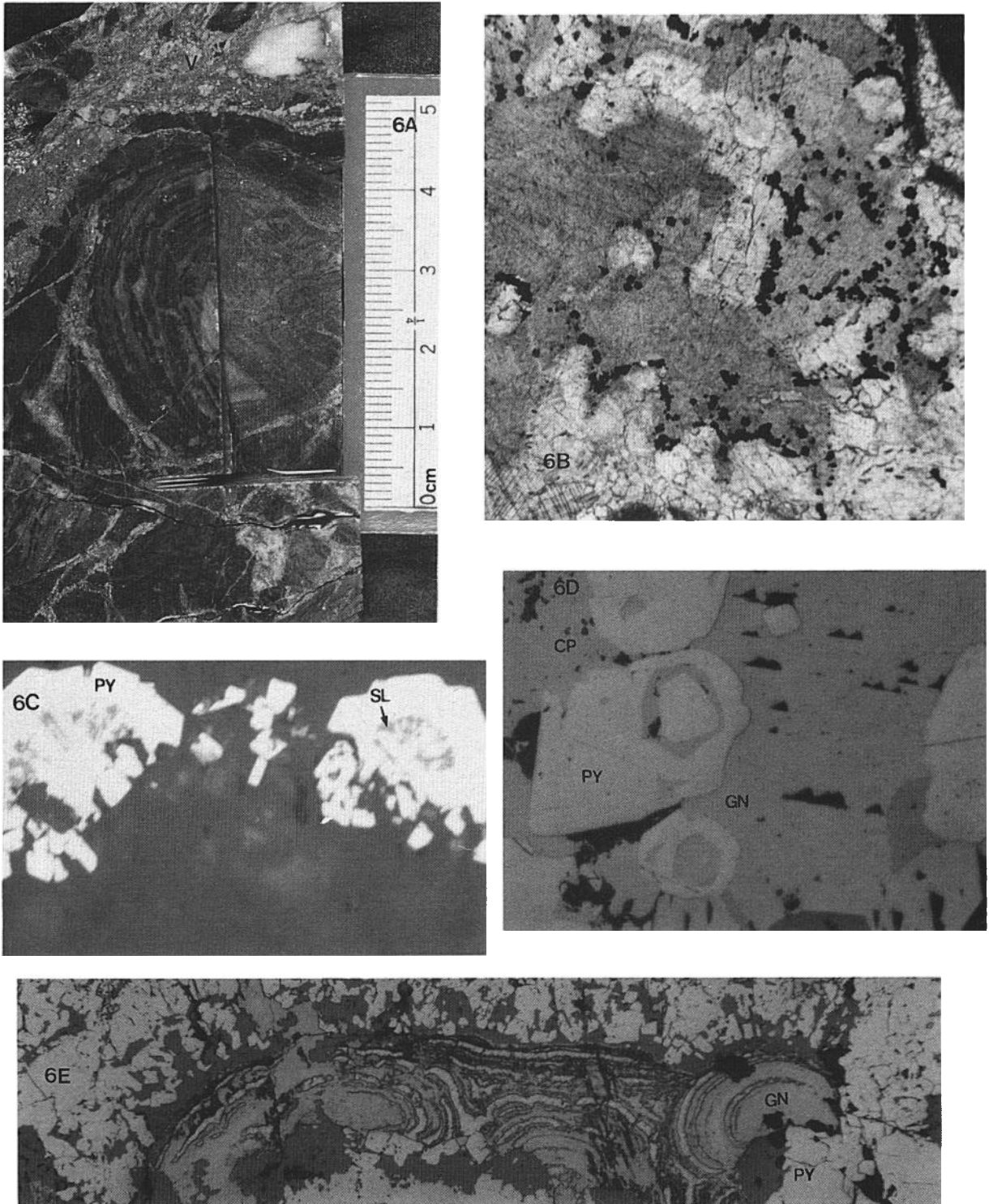


FIG. 6. Photographs of rocks and polished thin sections. Blende property, Yukon Territory. A. Mineralized stromatolite (drill hole 91-19, 78.6 m; marker G) contains sphalerite, pyrite, and lesser galena that follow stromatolite laminae (S) which are cut by veins (V). The sulfides following algal growth zones are syndepositional or formed during early diagenesis. B. Digitate cryptalgal laminae marked by botryoidal sulfide grains (SX: opaque) rimming growth zones (hole 91-60, 262 m). C. Close-up of the botryoidal sulfides in B, above (holes 91-60, 262 m). The sulfide botryoids show three stages of deposition: pyrite, pyrite with sphalerite, and pyrite. D. Botryoidal sulfide clusters (hole 91-60, 262 m) that occur close to later fractures are replaced and overgrown by other sulfides. E. Cryptalgal laminae completely replaced by pyrite (PY) and galena (GL; hole 91-41, 67.65 m).

TABLE 1. Homogenization Temperatures for Fluid Inclusions from the Blende Property, Yukon Territory

Sample no. ¹	Sample source	Temperature (°C)
MR1SL-P	DDH 91-45, 69.20 m	261
MR2SL-P	DDH 91-45, 69.20 m	288
MR3SL-P	DDH 91-45, 69.20 m	307
MR4SL-P	DDH 91-45, 69.20 m	291
MR5SL-P	DDH 91-45, 69.20 m	275
MR6SL-P	DDH 91-45, 69.20 m	284
MR7SL-U	DDH 91-45, 69.20 m	354
MR8SL-U	DDH 91-45, 69.20 m	359
MR9QZ-U	DDH 91-25, 67.10 m	158
MR10QZ-U	DDH 91-19, 76.30 m	196
MR11SL-U	DDH 91-45, 45.00 m	202
MR12SL-U	DDH 91-45, 45.00 m	205
MR13SL-U	DDH 91-45, 45.00 m	202
MR14SL-U	DDH 91-45, 45.00 m	216
MR15SL-U	DDH 91-45, 45.00 m	184
MR16SL-U	DDH 91-45, 45.00 m	106
MR17SL-P	DDH 91-45, 45.00 m	263
MR18SL-P	DDH 91-45, 45.00 m	264
MR19SL-P	DDH 91-45, 45.00 m	287
MR20SL-P	DDH 91-45, 45.00 m	293
MR21SL-P	DDH 91-45, 45.00 m	296

Heating stage was a USGS-type gas-flow, Fluid Inc. heating stage that was calibrated and is accurate to within ±0.1°C (T.J. Reynolds and K. Dunne, 1993, pers. commun.)

¹ QZ = quartz, P = primary, SL = sphalerite, U = uncertain

The inclusions homogenized to liquid between 261° and 307°C (Fig. 7A). Large (about 50 µm), isolated inclusions found in unzoned sphalerite were also interpreted as primary inclusions (Table 1, samples MR17SL-P to MR21SL-P). They homogenized to liquid between 263° to 296°C (Fig. 7A). The mean temperature of homogenization for all primary inclusions is 283° ± 5°C (standard error of the mean).

Inclusions of uncertain origin homogenized over a broader range in two groups (Table 1, Fig. 7B). One group that included inclusions located both in sphalerite and quartz homogenized over a range of 158° to 216°C with a mean temperature of 184° ± 12°C. The second group of only two inclusions homogenized at an unusually high temperature around a mean of 357° ± 2°C.

Pressure corrections to the data are probably minimal. The upper Gillespie Lake Group is unconformably overlain by postmineral carbonate strata of the Pinguicula Group. The implication is that upper Gillespie Lake Group dolostones probably were exposed to erosion during mineralization.

The primary fluid inclusion homogenization temperature is high compared to most described Mississippi Valley-type deposits (100°-150°C; Roedder, 1984). Because pressure corrections are minimal, temperatures of homogenization for primary inclusions apparently reflect temperatures of mineralization (283°C). The lower temperature inclusions (184°C) of uncertain origin may be a cooler part of the 283°C population. If so, it might reflect cooling of the hydrothermal system over time. Alternatively, the lower temperature inclusions could reflect

later metamorphism. The highest homogenization temperature (357°C) may be related to intrusion of the diorite sills.

Sulfur Isotopes

Samples of sphalerite, galena, pyrite, chalcopyrite, and tetrahedrite were handpicked for sulfur isotope analysis from mineralized drill core and surface specimens. In addition, five widely spaced samples of unmineralized dolostone from unit PGL₂ were analyzed for the isotopic composition of the total sulfur contained within the rock. Twenty-eight sulfur isotope analyses are in Table 2 that also contains analytical details.

Whole-rock analyses of unmineralized samples from unit PGL₂ group tightly around an average δ³⁴S value of 23.6 ± 0.4 per mil (standard error of the mean; Fig. 8), with values ranging from 22.6 to 24.8 per mil. These val-

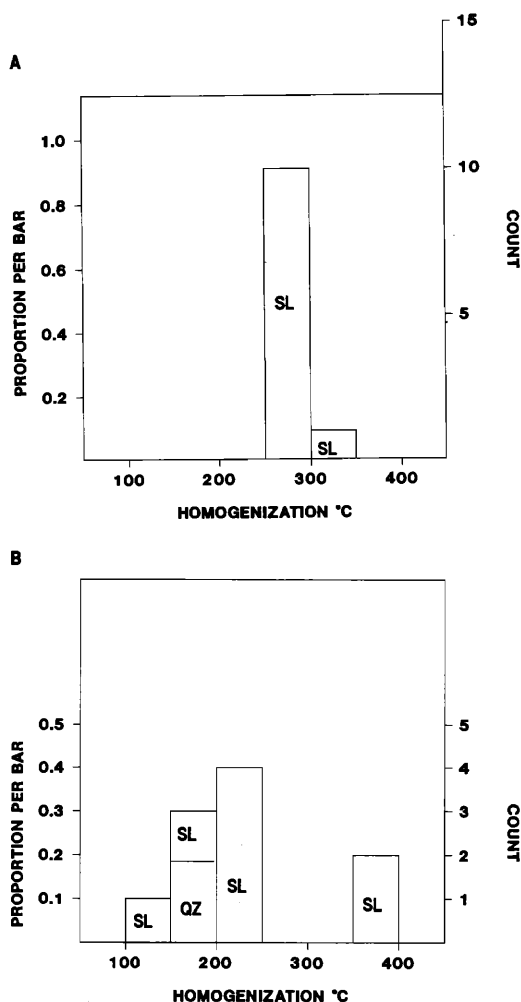


FIG. 7. Homogenization temperatures for fluid inclusions, Blende property, Yukon Territory (data are in Table 1). A. Homogenization temperatures for primary inclusions in sphalerite (SL). Mean is 283° ± 5°C (standard error of the mean). B. Homogenization temperatures for inclusions of uncertain type in sphalerite (SL) and quartz (QZ). Two groups are apparent. The lower temperature homogenization temperatures average 184° ± 2°C.

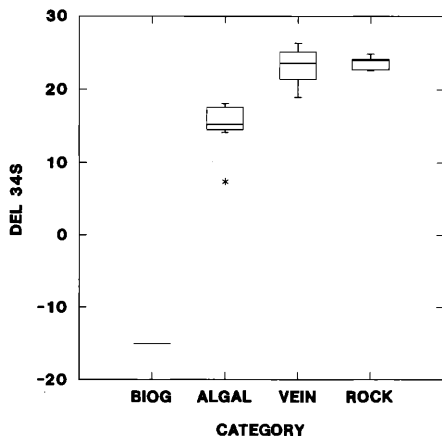


FIG. 8. Box plots showing the distribution of $\delta^{34}\text{S}$ ratios for different sulfide occurrences and whole-rock analyses, Blende property, Yukon Territory (data are in Table 2). ALGAL = sulfide sulfur isotope analyses from sulfides in stromatolitic horizons. Mean is 15.0 ± 1.2 (standard error of the mean). BIOG = single sulfur isotope analysis of a pyrite nodule from an algal zone. Value is -15.1 . VEIN = sulfide sulfur isotope analyses from sulfide veins hosted in dolomitites and dolarenites. Mean is 23.2 ± 0.9 . ROCK = bulk sulfur isotope analysis on unmineralized whole rock. Mean is 23.6 ± 0.4 . The mean $\delta^{34}\text{S}$ ratios for whole-rock and vein sulfides are indistinguishable. Sulfides hosted in stromatolites are isotopically shifted by about -8 to 15 per mil. These intermediate values apparently reflect a mixed sulfur source of dominantly anhydrite in rock (23%) and minor biogenic sulfide (-15%). Boxes define median and quartile values; whiskers and asterisks mark outside and extreme values, respectively.

ues are notably close to estimates of the sulfur isotope composition of evaporites (and therefore the ocean) during the Middle Proterozoic (Olson, 1984: $\delta^{34}\text{S} = 23.2\%$; Robinson and Ohmoto, 1973: $\delta^{34}\text{S} = 25.0\%$). For this reason, we conclude that the source of sulfur in unmineralized Blende dolostone is probably minor anhydrite. This is consistent with the results of Ueda et al. (1987), who were able to demonstrate that most carbonate rocks contain trace sulfate, and locally, trace sulfide. They showed that whole-rock sulfur isotope analyses may be used to estimate the isotopic composition of the ocean where evaporite data are not available. Unfortunately, rocks from the Blende property are too fine grained to confirm the presence of anhydrite petrographically, and amounts greater than 5 percent are required to detect it by X-ray diffraction methods.

The heaviest population of sulfide sulfur isotope data groups around an average $\delta^{34}\text{S}$ value of 23.2 ± 0.9 per mil (Vein category, Fig. 8) for veins hosted in dolosiltite. This is effectively identical to the average $\delta^{34}\text{S}$ value of 23.6 ± 0.4 per mil for the host dolostone. Sulfur for the veins apparently has a seawater or anhydrite source.

The lightest sulfide sulfur isotope measurement comes from a 0.5-cm pyrite blob in the middle of a large stromatolite (Biog category, Fig. 8). This pyrite has a negative $\delta^{34}\text{S}$ value of about -15 per mil, or 38 per mil lower than the estimated composition of mid-Proterozoic seawater. Sulfides formed from bacterially reduced sulfate typically have $\delta^{34}\text{S}$ values that are 15 to 25 per mil lower than the sulfur source and may theoretically reach fractionations

of 74 per mil (Sangster, 1976). Thus, the value of $\delta^{34}\text{S} = -15$ per mil is within the range caused by bacterial reduction.

Stromatolite units, generally associated with extensive ooid or pisoid beds (markers B and C, Fig. 3; marker F, Fig. 4), host sulfides with intermediate $\delta^{34}\text{S}$ values averaging 15.0 ± 1.2 per mil (Mixed category, Fig. 8). These intermediate values apparently reflect a mixed sulfur source with a minor biogenic sulfide component (-15%) and a more abundant seawater sulfate, represented by the dolomite host-rock sulfate (23%) source. Figure 5B, C, and D illustrates how biogenic sulfides are replaced by later, isotopically heavier vein sulfides.

One sample (Table 2: CIG0219CP) of sulfide matrix breccia directly overlying a diorite sill has a $\delta^{34}\text{S}$ value of 20.6 per mil. This is close to the estimated value for Proterozoic seawater or dolomite. Because this and other values are distinct from primitive magmatic sulfur ($\delta^{34}\text{S} = 0\%$), the diorite was not an important source of sulfur for Blende mineralization.

Carbon and Oxygen Isotopes

Five samples of dolostone from the upper Gillespie Lake Group (Figs. 3 and 4: unit G₂), one sample of diagenetic vein dolomite from unmineralized stromatolitic dolostone, and eight samples of sparry dolomite from mineralized veins were collected for carbon and oxygen isotope analysis. The carbon and oxygen isotope results are given in Table 3; analytical details are in the footnotes.

Dolomite whole rock (Whole rock in Table 3 and Fig. 9) has $\delta^{18}\text{O} = 23.1 \pm 0.5$ (standard error of the mean) and $\delta^{13}\text{C} = 2.3 \pm 0.3$ per mil. Dolomite spar associated with mineralization (spar mineralization in Table 3 and Fig. 9) has $\delta^{18}\text{O} = 19.9 \pm 0.5$ and $\delta^{13}\text{C} = 0.22 \pm 0.22$ per mil.

The calculated composition of fluid in equilibrium with the spar mineralization at 283°C (the mean homogenization temperature of primary inclusions) averages $\delta^{18}\text{O} = 13.5 \pm 0.5$ and $\delta^{13}\text{C} = 2.3 \pm 0.2$ per mil (calculated spar fluid, Fig. 9; carbon is calculated using the fractionation factor given by Ohmoto, 1972, for $\text{H}_2\text{CO}_{3\text{apparent}}$ at 300°C ; oxygen is calculated from the fractionation equation in Matthews and Katz, 1977, at 283°C). The average calculated composition of $\delta^{13}\text{C}$ in spar fluid is indistinguishable from that of the whole rock.

Whole rock and dolomite spar associated with vein mineralization form a linear trend in Figure 9, the plot of $\delta^{13}\text{C}$ versus $\delta^{18}\text{O}$. This trend is compatible with partial dissolution of original rock dolomite and precipitation of resulting lighter isotopes in the subsequent spar. Such linear trends between mineralized and nonmineralized dolomites is typical of other carbonate-hosted deposits (cf. Taylor, 1974). It also indicates that only one period of mineralization can be recognized and that the stable isotopes in host rocks and the ore-stage sparry dolomite are related genetically.

Calculated compositions of the spar-generating fluid are isotopically shifted to lower $\delta^{18}\text{O}$ and higher $\delta^{13}\text{C}$ values. Mineralizing fluid types compatible with $\delta^{18}\text{O} = 13.5$ and $\delta^{13}\text{C} = 2.3$ per mil are basinal brines and metamorphic

TABLE 2. Sulfur Isotope Data for the Blende Property, North-Central Yukon Territory

Sample no. ¹	Trial ²	Sample location	$\delta^{34}\text{S}_{\text{CDT}}$ ³ (‰)	Category ⁴
CIG0171GL		DDH 91-25, 67.10 m	24.0	Vein
CIG0171SL		DDH 91-25, 67.10 m	26.0	Vein
CIG0172GL		DDH 91-45, 69.20 m	23.4	Vein
CIG0172PY		DDH 91-45, 69.20 m	23.7	Vein
CIG0172SL		DDH 91-45, 69.20 m	26.3	Vein
CIG0173GL	1	DDH 91-45, 101.25 m	14.3	Algal
CIG0173GL	2	DDH 91-45, 101.25 m	13.9	Algal
CIG0173GL	Avg2	DDH 91-45, 101.25 m	14.1	Algal
CIG0173PY	1	DDH 91-45, 101.25 m	-14.6	Biogenic
CIG0173PY	2	DDH 91-45, 101.25 m	-15.5	Biogenic
CIG0173PY	Avg2	DDH 91-45, 101.25 m	-15.1	Biogenic
CIG0173SL	1	DDH 91-45, 101.25 m	17.9	Algal
CIG0173SL	2	DDH 91-45, 101.25 m	18.3	Algal
CIG0173SL	Avg2	DDH 91-45, 101.25 m	18.1	Algal
CIG0218PY		DDH 91-47, 152.6 m	7.4	Algal
CIG0218SL		DDH 91-47, 152.6 m	17.4	Algal
CIG0219CP		DDH 91-33, 377 m	20.6	Vein ⁵
CIG0220PY	1	DDH 91-41, 37.80 m	17.7	Algal
CIG0220PY	2	DDH 91-41, 37.80 m	17.8	Algal
CIG0220PY	Avg2	DDH 91-41, 37.80 m	17.8	Algal
CIG0221PY		20,100 N, 12,700 E	19.0	Vein
CIG0221SL		20,100 N, 12,700 E	22.3	Vein
CIG0227CP	1	DDH 91-60, 262.14 m	14.9	Algal
CIG0227CP	2	DDH 91-60, 262.14 m	14.8	Algal
CIG0227CP	Avg2	DDH 91-60, 262.14 m	14.8	Algal
CIG0227GL		DDH 91-60, 262.14 m	15.4	Algal
CIG0228TT		DDH 91-60, 261.54 m	15.1	Algal
CIG0222WR		Stromatolites	24.8	Rock
CIG0223WR		Stromatolites	24.0	Rock
CIG0224WR	1	Cryptobiogenic laminates	22.1	Rock
CIG0224WR	2	Cryptobiogenic laminates	25.6	Rock
CIG0224WR	Avg2	Cryptobiogenic laminates	23.9	Rock
CIG0225WR		Oolitic dolarenite	22.7	Rock
CIG0226WR		Molar tooth ⁶	22.6	Rock

¹ CP = chalcopyrite, GL = galena, PY = pyrite, SL = sphalerite, TT = tetrahedrite, WR = whole rock

² Avg2 = average of the two analyses immediately above; this average value is used in Figure 9

³ Samples were analyzed at H.R. Krouse's Stable Isotope Laboratory, Physics Department at the University of Calgary, Alberta, Canada; sulfur isotope results are reported relative to the Canyon Diablo troilite standard (CDT); error at 2 σ is less than 0.5 per mil; one whole-rock analysis was done using Kiba reagent; however, the other whole-rock samples were so anomalously rich in sulfur that direct burning liberated sufficient gas for isotopic analysis

⁴ Subdivision of type of material, as plotted in Figure 8

⁵ Sample was taken immediately above diorite sill

⁶ This texture in dolostone could have formed by subaqueous synaeresis dehydration at the sediment water interface (A. Donaldson, pers. commun., 1991) or by an organo-sedimentary process (O'Connor, 1972)

water. However, the $\delta^{18}\text{O}$ values fall outside the ranges for ocean water, meteoric water, magmatic water, formation waters, and ore fluids typical of Mississippi Valley-type deposits (Fritz, 1976). Therefore, this is additional support for a basal brine origin for the mineralizing fluids on the Blende property.

Galena Lead Isotopes

Galena samples were handpicked from drill core and hand specimens from all areas of the Blende property. Ga-

lena lead isotope ratios, measured for 13 samples, are in Table 4, which also contains analytical details.

Lead isotope signatures for most carbonate-hosted deposits in the Canadian Cordillera either conform to the shale curve (Godwin and Sinclair, 1982) or exhibit markedly radiogenic lines (Godwin et al., 1982; Morrow and Cumming, 1982) that intersect the shale curve. The intersection point of markedly radiogenic lines with the shale curve dates the mineralization (Godwin et al., 1988).

Data from the Blende deposit cluster between 1.5 and 1.4 Ga on the shale curve and depart from it along a line in Figure 10. This line is characteristic of the markedly radiogenic lines or anomalous lead lines (Russell et al., 1966), associated with Mississippi Valley-type deposits in the central United States (Heyl, 1969; Doe and Delevaux, 1972; Heyl et al., 1974; Crocetti et al., 1988). The lead is clearly upper crustal (Doe and Zartman, 1979) or of shale origin because all data points plot close to the curve of the shale model marked by asterisks in Figure 9. It does not have a recognizable mantle component that would indicate a direct contribution from the diorite sills.

The age of mineralization defined by the intersection in Figure 10 of the markedly radiogenic line and the shale curve (asterisks) on the $^{208}\text{Pb}/^{204}\text{Pb}$ vs. $^{206}\text{Pb}/^{204}\text{Pb}$ and the $^{207}\text{Pb}/^{204}\text{Pb}$ vs. $^{206}\text{Pb}/^{204}\text{Pb}$ plots is about 1.5 Ga. Another estimate is available in the $^{208}\text{Pb}/^{206}\text{Pb}$ vs. $^{207}\text{Pb}/^{206}\text{Pb}$ plot in Figure 10 (this plot is more robust because the ^{204}Pb error is removed). All three plots indicate an age of about 1.5 Ga. However, the tangential intersection of the markedly radiogenic line with the shale curve allows an interpretation as young as 1.4 Ga, which would correspond to the uranium-lead zircon age of the sills (1.38 Ga, above). For reasons cited elsewhere we favor the younger age interpretation.

Discussion

Source of metals

The major source of metals for the Blende deposit is most probably shales of the Quartet Group or shaly members of the lower Gillespie Lake Group. Lead isotope data indicate lead was mostly derived from upper crustal rocks, such as shales, with minor contamination by anomalously radiogenic lead; the diorite was not a source for the metals. We assume that the lead source was also the main source of zinc, silver, and copper. The calculated values for the stable isotopes of carbon and oxygen in the mineralizing fluids also are characteristic of basal brines.

A minor metal source could be the upper Gillespie Lake Group, which is the host rock to the mineralization. Some pyrite, and possibly sphalerite, appears to have been deposited during sedimentation (Fig. 6B and C).

Thus, we envisage that metal chloride-rich stratafugic brine solutions were expelled from shaly units during burial, compaction, and maturation (Beales and Jackson, 1968). A small markedly radiogenic component to the lead could have been added during transport of the expelled brines through sandier aquifers. For example, most sandstones contain elevated amounts of zircon, which

TABLE 3. Carbon and Oxygen Isotope Results (‰) from the Blende Property, Yukon Territory

Sample no. ¹	Sample source ²	$\delta^{13}\text{C}_{\text{PDP}}$	$\delta^{13}\text{C}_{\text{H}_2\text{CO}_3}$ ³	$\delta^{18}\text{O}_{\text{V-SMOW}}$	$\delta^{18}\text{O}_{\text{carb-water}}$ ⁴
Whole rock					
CIO0223DO	Diagenetic do vein	1.95		21.07	
CIG0222WR	Strom do	4.21		25.11	
CIG0223WR	Strom do	2.50		25.00	
CIG0224WR	Cryptobio do	2.00		22.69	
CIG0225WR	Oolitic do-arenite	1.67		22.97	
CIG0226WR	Molar Tooth do	1.86		22.32	
Spar mineralization					
CIG0171DO	DDH 91-25, 67.10 m	-0.11	1.99	19.56	14.2
CIG0172DO	DDH 91-45, 69.20 m	-0.44	1.66	17.74	11.3
CIG0173DO	DDH 91-45, 101.25 m	-0.31	1.79	18.44	12.0
CIG0218DO	DDH 91-47, 152.6 m			20.09	13.5
CIG0220DO	DDH 91-41, 37.80 m	0.41	2.51	20.50	13.9
CIG0221DO	20,100 N, 12,700 E	0.65	2.75	20.59	14.0
CIG0227DO	DDH 91-60, 262.14 m	1.18	3.28	22.24	15.7
CIG0228DO	DDH 91-60, 261.54 m	0.13	2.23	19.77	13.2

Samples were analyzed at H.R. Krouse's Stable Isotope Laboratory, Physics Department at the University of Calgary, Alberta, Canada; carbon and oxygen isotope results were reported relative to the PeeDee Chicago belemnite standard (PBD CO_2); the oxygen isotope data are converted to the Vienna Standard Mean Ocean Water (V-SMOW) scale (Coplen et al., 1983): $\delta^{18}\text{O}_{\text{V-SMOW}} = 1.03091/\delta^{18}\text{O}_{\text{PDP}} + 30.91$; Error at 2σ is less than 0.2 per mil

¹ DO = dolomite, WR = whole rock

² Strom = stromatolitic, Cryptobio = cryptobiogenic laminate

³ $\delta^{13}\text{C}$ is calculated composition of the spar-generating fluid using the fractionation factor given by Ohmoto (1972) for H_2CO_3 apparent at 300°C

⁴ $\delta^{18}\text{O}_{\text{carb-water}}$ is calculated composition of the spar-generating fluid calculated from the equation in Matthews and Katz (1977) at 283°C

contains uranium and therefore produces markedly radiogenic lead that can be leached into brines.

Fluid transport

Much mineralization is focused along normal fault zones. These faults are obvious pathways into the upper Gillespie Lake Group for upwardly migrating metal-rich brines. It is likely that the sills are associated with a rifting event. Such areas of extension commonly are marked by high heat flow. This is apparently reflected in the high temperatures found in the fluid inclusions.

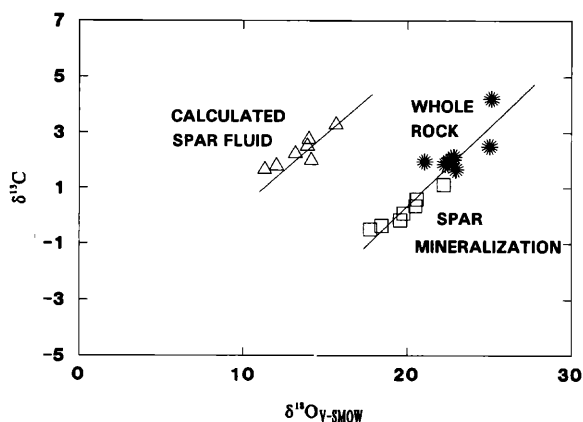


Fig. 9. $\delta^{18}\text{O}$ versus $\delta^{13}\text{C}$ for whole-rock (asterisks), dolomite spar associated with mineralization (squares), and mineralizing fluid calculated from spar (triangles), Blende property, Yukon Territory. Data are in Table 3; size of data symbols approximates data error. The whole-rock values are typical of marine carbonates. The trend between spar associated with mineralization and nonmineralized whole-rock dolomite is typical of carbonate-hosted deposits.

Along the normal faults, pyrite, sphalerite, and galena replace the wall rock directly (Fig. 5B). However, significant mineralization preferentially follows certain oolitic and stromatolite beds within unit PGL₂, because they were more permeable.

Ore deposition

The following features seem particularly important to ore deposition in the Blende deposit:

TABLE 4. Galena Lead Isotope Data for the Blende Property, North-Central Yukon Territory

Sample no. ¹	$^{206}\text{Pb}/^{204}\text{Pb}$	$^{207}\text{Pb}/^{204}\text{Pb}$	$^{208}\text{Pb}/^{204}\text{Pb}$	$^{207}\text{Pb}/^{206}\text{Pb} \cdot 100$	$^{208}\text{Pb}/^{206}\text{Pb} \cdot 10$
10139-001	16.581	15.477	36.378	93.342	21.940
10139-002	16.382	15.439	36.060	94.246	22.012
10139-003	16.358	15.432	36.042	94.342	22.033
10139-004	16.377	15.444	36.070	94.303	22.025
10139-005Avg2	16.507	15.444	36.224	93.559	21.945
10139-006Avg2	16.432	15.440	36.090	93.965	21.964
10139-007	16.349	15.432	36.023	94.387	22.034
10139-008Avg2	16.321	15.401	35.966	94.354	22.037
10139-009Avg2	17.008	15.501	36.578	91.141	21.507
10139-010Avg2	16.841	15.493	36.687	91.994	21.785
10139-011Avg2	16.450	15.435	36.112	93.829	21.954
10139-012Avg2	16.555	15.452	36.270	93.340	21.910
10139-013Avg2	16.565	15.467	36.310	93.368	21.919

Most samples were analyzed by Anne Pickering, Geochronometry Laboratory, Department of Geological Sciences, University of British Columbia, Vancouver, B.C., Canada; Analysis of 10139-001 is from LEADTABLE (Godwin et al., 1988); a Vacuum Generators Ltd. Isomass 54R solid source, single filament (silica gel method), mass spectrometer was used; Errors at 2σ are less than 0.01 percent

¹ Avg2 is the average of two separate analyses from the same specimen

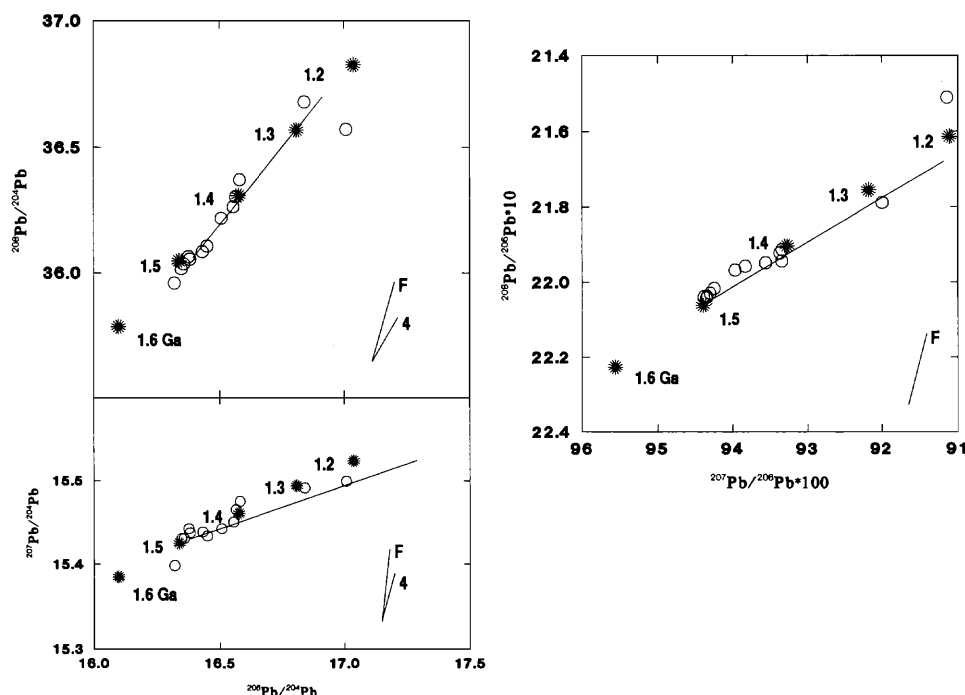


FIG. 10. Galena lead-lead plot of data (Table 4), for the Blende property, Yukon Territory. Blende data model at about 1.5 Ga on the $^{208}\text{Pb}/^{204}\text{Pb}$ vs. $^{206}\text{Pb}/^{204}\text{Pb}$ plot, and $^{207}\text{Pb}/^{204}\text{Pb}$ vs. $^{206}\text{Pb}/^{204}\text{Pb}$ plots. The $^{208}\text{Pb}/^{206}\text{Pb}$ vs. $^{207}\text{Pb}/^{206}\text{Pb}$ plot removes ^{204}Pb error and indicates a potential deposit age range of 1.4 to 1.5 Ga. F = trend of fractionation error, 4 = trend of ^{204}Pb error. Size of data symbols approximates data error. Asterisks, with dates in Ga, mark the shale curve of Godwin and Sinclair (1982); this is an upper crustal model specific to the Canadian Cordillera.

1. The sills may have caused the high temperatures reflected by the fluid inclusions in the mineralization (near 300°C), but otherwise the mineralization is not directly related to the sills. Fluid inclusions are low to moderate salinity (no daughter minerals); if the mineralizing fluid had a magmatic or metamorphic component, high-salinity and/or CO_2 -rich inclusions should be present. Sulfur and galena lead isotopes also do not support a magmatic component to the mineralization.

2. The dolomite host to mineralization is sulfur rich, as determined during sulfur isotope analyses (see footnote 3, Table 2). Most of the sulfur in the rock probably occurs as anhydrite.

3. Stromatolitic horizons and adjacent oolitic units are associated with much of the mineralization (Figs. 3 and 4). These form excellent mineralization traps (cf. Ran Chongying, 1989) because they are permeable, can contain abundant anhydrite because of their shallow formation, are made of abundant organic carbon, and host minor amounts of biogenic sulfide. The organic material can be thermally altered to the reductant methane, and the anhydrite can be a source of sulfur for sulfide.

4. The sulfur isotope values (Fig. 8) in the mineralization is related closely to the seawater sulfate signature of the host stromatolitic dolostone. Sulfur isotopes in veins are nearly identical to the rock sulfur ($\delta^{34}\text{S} = 23\text{--}24\text{‰}$). Mineralization along the stromatolitic horizon has slightly lower sulfur isotope values ($\delta^{34}\text{S} = 15\text{‰}$), apparently due

to mixing with minor synsedimentary, biogenic sulfide ($\delta^{34}\text{S} = -15\text{‰}$).

5. The carbon and oxygen isotopes in the host rocks and the ore-stage sparry dolomite are related genetically. Both are related to ancient seawater.

Most mineralization at the Blende deposit has the following paragenesis (Fig. 5A, B, and C): brucite needles in vein envelopes, galena followed by sphalerite in veins, and sparry dolomite in the core of veins greater than 0.5 cm wide. Sphalerite abundance is greater than galena. Pyrite is more abundant than chalcopyrite and together account for less than 10 percent of the deposit. Using the PATH program (written by T.H. Brown and E. Perkins, Department of Geological Sciences, University of British Columbia), a mineralizing solution was devised such that, when reacting with Blende dolostone, it would produce the paragenesis and relative abundance of minerals at the Blende deposit, as above.

PATH uses the concept of Helgeson et al. (1970) in which a reaction path is followed by addition of a small amount of reactant(s) to a system at equilibrium. Cumulative changes in the amount of each component and species in the system are recalculated after each addition of reactant(s). One limitation to PATH is that it does not model flow of a fluid with changing composition as it moves spatially through a rock. However, the run below for a continuous reaction of a likely hydrothermal fluid with a host rock of organic- and anhydrite-bearing carbonate, and

TABLE 5. Rock and Water Characteristics Used in Modeling with PATH, Blende Zn-Pb-Ag Deposit, North-Central Yukon Territory

Rock ¹		Water (280°C)	
Mineral	Reaction coefficient	Ion ²	Molality
Dolomite	0.95	Ca ²⁺	0.13E-3
Anhydrite	0.30	Mg ²⁺	0.23E-4
Methane	0.20	PbCl ₄ ²⁻	0.11E-4
		ZnCl ₄ ²⁻	0.61E-4
		SO ₄ ²⁻	0.11E-5
		Cl ⁻	0.25E + 1
		Na ⁺	0.25E + 1
		HS ⁻	0.15E-5
		H ₂ S	0.78E-6
		H ₂ CO ₃	0.24E-3
		HCO ₃ ⁻	0.39E-4
		Mg(OH) ⁺	0.11E-3
		pH	6.8

¹ Blende dolomite is approximated by a mixture of dolomite and anhydrite; the contained organic matter is approximated by the mineral methane.

² Only solution species with molality > 10⁻⁶ are reported

subsequent reaction products, reasonably approximates the mineral paragenesis at the Blende deposit.

Rock and water characteristics that were used in the PATH model are defined in Table 5. The host-rock reactant, Blende dolostone, is composed chiefly of dolomite, anhydrite, and a minor algal organic (including trace shale) component. Thus, the host reactant was approximated by dolomite (95 wt %) and minor anhydrite. The shale component was omitted from the simulation for simplicity. Metal chloride complexes were assumed to be in the mineralizing fluid, following the characteristics of metal-bearing brines proposed by Beales and Jackson (1968). Characteristics of the fluid generating Blende mineralization include a metal content of 10 to 100 ppm Pb + Zn and negligible sulfate and sulfide. The temperature used for the simulation was 280°C, about the temperature of mineralization estimated from primary inclusions in sphalerite (Fig. 7A).

Most models by others suggest brine transport of either sulfate or sulfide—usually sulfate with reduction to sulfide at the mineralizing site (cf. Anderson, 1991). However, we believe that in the latter case the sulfur isotopes in the mineralization would not relate directly to the sulfur isotopes in the host rock, as they do at the Blende. There is debate on whether or not direct thermochemical reduction of sulfate is fast enough to provide sulfide for in situ deposition. However, as pointed out in Anderson (1991), thermochemical reduction of sulfate above 80°C is an accepted fact in the petroleum literature (e.g., Krouse et al., 1988). In the PATH analysis, below, we have accepted that direct sulfate reduction of anhydrite did occur—based mainly on sulfur isotope evidence.

Simulation of Blende mineralization by a PATH run is presented in Table 6 and reveals the following:

1. Dolomite [CaMg(CO₃)₂], anhydrite [CaSO₄], and

methane [CH₄] are consistent reactants in all of the important reactions 1 to 5.

2. Sulfate in anhydrite is reduced to sulfide (reactions 1 to 5) in the presence of methane, but dolomite is an integral part of all the reactions.

3. By the time galena and sphalerite are precipitated (reactions 2 and 3) there is available sulfide from earlier reduction of sulfate in anhydrite (reaction 1), but most of the sulfide for the sulfide precipitation comes from continued reduction of sulfate in anhydrite.

4. Calcite and dolomite spar (reactions 4 and 5) are formed mainly by the dissolution and reprecipitation of dolomite and anhydrite. This is compatible with the intimate relationship, based on carbon and oxygen isotopes (Fig. 9), of the host dolomite with ore-stage sparry dolomite.

5. In the simulation the minerals are precipitated in the same order as the paragenesis observed, namely: early formation of brucite (Mg(OH)₂: reaction 1) observed in vein envelopes, sequential precipitation of galena (PbS: reaction 2) and sphalerite (ZnS: reaction 3) seen in veins, and late precipitation of dolomite (CaMg(CO₃): reaction 5) occurring as sparry vein infillings. Earlier formed brucite and calcite (e.g., reaction 4) can be dissolved by reaction 5; this could explain why brucite and calcite were not observed in the veins. The predicted association of late sphalerite with sparry dolomite was not observed clearly in the mineralization.

TABLE 6. List of Simplified Important Reactions, as Modeled by PATH, between the Upper Gillespie Lake Group Dolostone and the Mineralizing Fluid

Reactants	Products
Reaction 1: Precipitate brucite 0.95CaMg(CO ₃) ₂ + 0.03CaSO ₄ →	1.39Mg(OH) ₂ + 0.98Ca ²⁺ + 0.01SO ₄ ²⁻ + 0.02HS ⁻ + 0.005H ₂ S + 1.50H ₂ CO ₃ + 0.01OH ⁻ + 0.41HCO ₃ ⁻
Reaction 2: Precipitate galena 0.95CaMg(CO ₃) ₂ + 0.03CaSO ₄ →	1.18Mg(OH) ₂ + 0.98Ca ²⁺ + 0.01SO ₄ ²⁻ + 0.08Cl ⁻ + OH ⁻ + 1.3H ₂ CO ₃ + 0.625HCO ₃ ⁻ + 0.02PbS
Reaction 3: Precipitate sphalerite 0.95CaMg(CO ₃) ₂ + 0.03CaSO ₄ →	1.06Mg(OH) ₂ + 0.98Ca ²⁺ + 0.01SO ₄ ²⁻ + 0.12Cl ⁻ + 0.99OH ⁻ + 1.14H ₂ CO ₃ + 0.78HCO ₃ ⁻ + 0.03ZnS
Reaction 4: Precipitate calcite and sphalerite 0.95CaMg(CO ₃) ₂ + 0.03CaSO ₄ →	0.93Mg(OH) ₂ + 1.02Ca(CO ₃) ₂ + 0.01SO ₄ ²⁻ + 0.08Cl ⁻ + 0.02Mg(OH) ⁺ + 0.62HCO ₃ ⁻ + 0.02ZnS + 2.49H ⁺
Reaction 5: Precipitate dolomite and sphalerite, dissolve brucite and calcite 0.95CaMg(CO ₃) ₂ + 0.03CaSO ₄ →	0.97CaMg(CO ₃) ₂ + 0.01SO ₄ ²⁻ + 0.08Cl ⁻ + 0.06H ₂ O + 0.02ZnS + 0.02Ca ²⁺

Other PATH runs, not presented here, indicate the following:

1. With the conditions of Table 5, but without the presence of the mineral methane, sulfide was not precipitated. This emphasizes Barton's (1967) suggestion that sulfate reduction by methane could be the precipitating agent in Mississippi Valley-type deposits. This point has been amplified by Anderson (1991).
2. High temperatures used here are not necessary to obtain the mineral sequences described. Similar results were obtained at 100°C.
3. Pyrite precipitation immediately becomes important if the host rock is ferroan dolomite. This was modeled by considering a rock containing minor siderite as well as dolomite.
4. Similar mineral precipitation sequences can be obtained if the mineralizing brine contains significant concentrations of sulfate. Thus, PATH runs do not preclude the possibility that sulfate or sulfide was brought to the mineral deposition site with the metal-bearing brine, but the sulfur isotope data indicate that this is unlikely.

Conclusions

The geology, isotopic results, fluid inclusion data, and thermodynamic modeling constrain the origin of the Blende carbonate-hosted Zn-Pb-Ag deposit. Our model is a modification of the three-reservoir conceptual model of Beales and Jackson (1966), in which a basinal metal chloride brine mixes at the depositional site with separate sulfide-rich fluids generated elsewhere by bacterial reduction of anhydrite. Modifications of Beales and Jackson's model by others (see Anderson and Garvin, 1987, fig. 4) commonly impose fluid transportation of sulfide, sulfate, oxygen, and methane to the site of mineral deposition, in addition to metal brine transport. Our model for the Blende deposit differs somewhat from the above. We argue that the stratifugic metal chloride-bearing brine encounters a favorable host of dolomite, organics, and sulfate, converts the organics to methane and reduces the sulfate in the host rock to sulfide, and precipitates galena and sphalerite directly in favorable host-rock porosity of primary and solution origin.

Genesis of the Blende deposit can be summarized as follows: (1) formation of metal chloride brines from shales of the Quartet Group or shaly members of the lower Gillespie Lake Group, (2) expulsion of these stratifugic brines during compaction and maturation of the shales, (3) emplacement of these fluids upward, guided along normal faults associated with the thermal and extensional regime marked by the diorite sills, to algal dolomite horizons, (4) conversion of stromatolitic, organic carbon to methane by hot mineralizing fluids, (5) reaction by the hot mineralizing fluids and methane with anhydrite and the host dolomite to produce sulfide, and (6) sequential precipitation of galena, sphalerite then dolomite spar by reaction of the sulfide, etc., with the basinally derived metal chloride complexes.

Acknowledgments

R. Wallis of Billiton Metals Canada, Inc., generously provided funding for field and laboratory work. Funding was also received from an Arctic and Alpine research grant to C.G. Field support was given by Archer, Cathro and Associates (1981) Ltd. G. Abbott of the Department of Indian and Northern Affairs provided transportation for C.G. to the site and funding for the U-Pb analysis of zircon by M. Bevier, Geological Survey of Canada. Special thanks are extended to A. Donaldson and C. Roots for their timely visit to the Blende deposit. G. Lutes, D. Eaton, F. Gish, G. Evancio, and G. MacIntosh offered many interesting ideas and suggestions. J. Thompson and A. Sinclair helped with some interpretations. T. Brown provided a copy of the PATH program and guided our understanding of the results. We also thank A. Pickering, D. Runkle, and J. Harakal from the Geochronology Laboratory at the University of British Columbia. H.R. Krouse, Physics Department, University of Calgary, Alberta, Canada, generously provided the support of his laboratory in the stable isotope studies. Reviews of the manuscript by *Economic Geology* referees contributed substantially to this paper.

June 8, 1993; September 12, 1994

REFERENCES

- Anderson, G.M., 1991, Organic maturation and ore precipitation in southeast Missouri: *ECONOMIC GEOLOGY*, v. 86, p. 909-926.
- Anderson, G.M., and Garven, G., 1987, Sulfate-sulfide-carbonate associations in Mississippi Valley-type lead-zinc deposits: *ECONOMIC GEOLOGY*, v. 82, p. 482-488.
- Barton, P.B., 1967, Possible role of organic matter in the precipitation of the Mississippi Valley-type ores: *ECONOMIC GEOLOGY MONOGRAPH* 3, p. 371-378.
- Beales, F.W., and Jackson, S.A., 1968, Pine Point--a stratigraphic approach: *Canadian Institute of Mining and Metallurgy Bulletin*, v. 61, p. 867-878.
- Coplen, T.B., Kendall, C., and Hopple, J., 1983, Comparison of stable isotope reference samples: *Nature*, v. 302, p. 236-238.
- Crocetti, C.A., Holland, H.D., and McKenna, L.W., 1988, Isotopic composition of lead in galenas from the Viburnum trend, Missouri: *ECONOMIC GEOLOGY*, v. 83, p. 355-376.
- Delaney, G.D., 1981, The mid-Proterozoic Supergroup, Wernecke Mountains, Yukon Territory: *Canada Geological Survey Paper* 81-10, p. 1-24.
- Doe, B.R., and Delevaux, M.H., 1972, Source of lead in southeast Missouri galena ores: *ECONOMIC GEOLOGY*, v. 67, p. 409-425.
- Doe, B.R., and Zartman, R.E., 1979, Plumbo-tectonics I, the Phanerozoic. in Barnes, H.L., ed., *Geochemistry of hydrothermal ore deposits*, 2nd ed.: New York, NY, Wiley Interscience, p. 22-70.
- Eisbacher, G.H., 1981, Sedimentary tectonics and glacial record in the Windermere Supergroup, Mackenzie Mountains, northwestern Canada: *Canada Geological Survey Paper* 80-27, 40 p.
- Fritz, P., 1976, Oxygen and carbon isotopes in ore deposits in sedimentary rocks, in Wolf, K.H., ed., *Handbook of strata-bound and stratiform ore deposits*: New York, Elsevier, v. 2, p. 191-217.
- Godwin, C.I., and Sinclair, A.J., 1982, Average lead isotope growth curves for shale-hosted zinc-lead deposits, Canadian Cordillera: *ECONOMIC GEOLOGY*, v. 77, p. 675-690.
- Godwin, C.I., Sinclair, A.J., and Ryan, B.D., 1982, Lead isotope models for the genesis of carbonate-hosted Zn-Pb, shale-hosted Ba-Zn-Pb, and silver-rich deposits in the northern Canadian Cordillera: *ECONOMIC GEOLOGY*, v. 77, p. 82-94.
- Godwin, C.I., Gabites, J.E., and Andrew, A., 1988, LEADTABLE: A galena-lead isotope database for the Canadian Cordillera, with a guide

- to its use by explorationists: British Columbia Ministry of Energy, Mines and Petroleum Resources, Mineral Resources Division Paper 1988-4, 188 p.
- Green, L.H., 1972, Dawson, Larsen Creek and Nash Creek map areas, Yukon Territory: Canada Geological Survey Memoir 364, 157 p.
- Helgeson, H.C., Brown, T.H., Nigrini, A., and Jones, T.A., 1970, Calculation of mass transfer in geochemical processes involving aqueous solutions: *Geochimica et Cosmochimica Acta*, v. 34, p. 569-592.
- Heyl, A.V., 1969, Some aspects of zinc-lead-barite-fluorite deposits in the Mississippi Valley, U.S.A.: Institution of Mining and Metallurgy Transactions, v. 78, section B, p. B148-B160.
- Heyl, A.V., Landis, G.P., and Zartman, R.E., 1974, Isotopic evidence for the origin of Mississippi Valley-type mineral deposits: A review: *ECONOMIC GEOLOGY*, v. 69, p. 992-1006.
- Krouse, H.R., Viau, C.A., Eliuk, L.S., Ueda, A., and Halas, S., 1988, Chemical and isotopic evidence of thermochemical sulfate reduction by light hydrocarbon gases in deep carbonate reservoirs: *Nature*, v. 133, p. 414-419.
- Matthews, A., and Katz, A., 1977, Oxygen isotope fractionation during dolomitization of calcium carbonate: *Geochimica et Cosmochimica Acta*, v. 41, p. 1431-1438.
- Morrow, D.W., and Cumming, G.L., 1982, Interpretation of lead isotope data from zinc-lead mineralization in the northern part of the western Canadian Cordillera: *Canadian Journal of Earth Sciences*, v. 19, p. 1070-1078.
- Mustard, P.S., Roots, C.F., and Donaldson, J.A., 1990, Stratigraphy of the Middle Proterozoic Gillespie Lake Group in the southern Wernecke Mountains, Yukon: Canada Geological Survey Paper 90-1E, p. 43-53.
- O'Connor, M.P., 1972, Classification and environmental interpretation of molar tooth structure from the Late Precambrian Belt-Purcell Supergroup: *Journal of Geology*, v. 80, p. 592-610.
- Ohmoto, H., 1972, Systematics of sulfur and carbon isotopes in hydrothermal ore deposits: *ECONOMIC GEOLOGY*, v. 67, p. 551-578.
- Olson, R.A., 1984, Genesis of paleokarst and strata-bound zinc-lead sulfide deposits in a Proterozoic dolostone, northern Baffin Island, Canada: *ECONOMIC GEOLOGY*, v. 79, p. 1056-1103.
- Ran Chongying, 1989, Environmental significance of stromatolites and their relation to copper ore in the Luoxue Formation of the Kunyang Group in Dongchuan, Yunnan, China: Geological Association of Canada Special Paper 36, p. 679-685.
- Robinson, B.W., and Ohmoto, H., 1973, Mineralogy, fluid inclusions, and stable isotopes of the Echo Bay U-Ni-Ag-Cu deposits, Northwest Territories, Canada: *ECONOMIC GEOLOGY*, v. 68, p. 635-656.
- Roedder, E., 1984, Fluid inclusions: *Reviews in Mineralogy*, v. 12, 646 p.
- Roots, C.F., 1990, New geological maps for the southern Wernecke Mountains: Canada Geological Survey Paper 90-1E, p. 5-13.
- Russell, R.D., Kanasewich, E.R., and Ozard, J.M., 1966, Isotopic abundances of lead from a frequently-mixed source: *Earth and Planetary Science Letters*, v. 1, p. 85-88.
- Sangster, D.F., 1976, Sulfur and lead isotopes in strata-bound deposits, in Wolf, K.H., ed., *Handbook of strata-bound and stratiform ore deposits*: New York, Elsevier, v. 2, p. 219-265.
- Taylor, H.P., Jr., 1974, The application of oxygen and hydrogen isotope studies to problems of hydrothermal alteration and ore deposition: *ECONOMIC GEOLOGY*, v. 69, p. 843-883.
- Thompson, R.I., Mercier, E., and Roots, C.F., 1986, Extension and its influence on Canadian Cordilleran passive margin evolution: *Geological Society of London Special Publication*, v. 28, p. 409-420.
- Ueda, A., Campbell, F.A., Krouse, H.R., and Spencer, R.J., 1987, $^{34}\text{S}/^{32}\text{S}$ variations in trace sulphide and sulphate in carbonate rocks of a Devonian reef, Alberta, Canada, and the Precambrian Siyeh Formation, Montana, U.S.A.: *Chemical Geology*, v. 65, p. 383-390.